



Open camera or QR reader and scan code to access this article and other resources online.

A Rat Anti-Mouse CD39 Monoclonal Antibody for Flow Cytometry

Hiroyuki Suzuki, Tomohiro Tanaka, Yuma Kudo, Mayuki Tawara, Aoi Hirayama, Mika K. Kaneko, and Yukinari Kato

By converting extracellular adenosine triphosphate to adenosine, CD39 is involved in adenosine metabolism. The extracellular adenosine plays a critical role in the immune suppression of the tumor microenvironment. Therefore, the inhibition of CD39 activity by monoclonal antibodies (mAbs) is thought to be one of the important strategies for tumor therapy. In this study, we developed novel mAbs for mouse CD39 (mCD39) using the Cell-Based Immunization and Screening (CBIS) method. One of the established anti-mCD39 mAbs, C₃₉Mab-2 (rat IgG_{2a}, lambda), reacted with mCD39-overexpressed Chinese hamster ovary-K1 (CHO/mCD39) and an endogenously mCD39-expressed cell line (SN36) by flow cytometry. The kinetic analysis using flow cytometry indicated that the dissociation constant (K_D) values of C₃₉Mab-2 for CHO/mCD39 and SN36 were 5.5×10^{-9} M and 4.9×10^{-9} M, respectively. These results indicated that C₃₉Mab-2 is useful for the detection of mCD39 in flow cytometry.

Keywords: mouse CD39, monoclonal antibody, the Cell-Based Immunization and Screening, CBIS

Introduction

ADENOSINE-MEDIATED IMMUNOSUPPRESSION has been reported to be critical for tumor immune evasion. Various cancers showed the elevated expression of CD39 (ectonucleoside triphosphate diphosphohydrolase 1; encoded by *ENTPDI*), which hydrolyzes extracellular adenosine triphosphate (eATP) to adenosine diphosphate and adenosine monophosphate (AMP), promotes the local accumulation of adenosine surrounding tumors.¹ The adenosine-induced immunosuppression is mediated via four G protein-coupled type 1 purinergic (P1) receptors, A₁, A_{2A}, A_{2B}, and A₃ expressed on immune cells.² The A_{2A} and A_{2B} are G_S-coupled receptors and trigger intracellular cAMP accumulation among the four P1 receptors. The cAMP signaling mediates immunosuppression by activation of effectors including protein kinase A.³

The immunosuppressive effects of the A_{2A} receptor *in vivo* were first reported by Sitkovsky's group.⁴ Inflammatory stimuli that caused minimal tissue damage in wild-type mice were sufficient to induce extensive tissue damage, higher levels of proinflammatory cytokines, and individual death in mice lacking the A_{2A} receptor.⁴ They also showed genetic evidence of the importance of the A_{2A} receptor in tumor immunity.⁵ These findings indicated that the critical roles in

CD39–adenosine–A_{2A} receptor axis in antitumor immunity and several landmark studies have developed multiple strategies targeting adenosine metabolism.^{6,7}

The development of anti-CD39 monoclonal antibodies (mAbs) is one of the strategies to modulate adenosine metabolism. A preclinical study revealed that an anti-mouse CD39 (mCD39) mAb (clone B66), which inhibits mCD39 activity *in vitro*, exhibited the antitumor effect in syngeneic models by the monotherapy and combination therapy with the programmed cell death-1 (PD-1) blockade.⁸ They also showed that B66 triggers an eATP–P2X7–inflammation–interleukin-18 (IL-18) pathway that promotes tumor immunity, and overcomes the resistance of PD-1 blockade.⁸ The anti-human CD39 mAbs, such as TTX-030, IPH5201, and SRF-617, were designed to suppress the enzymatic activity of CD39 with minimizing Fc receptor-mediated engagement to avoid the side effects.^{8,9} These mAbs have entered the clinical trials for solid tumors with a combination of immune checkpoint inhibitors or chemotherapeutic agents.⁶

We have established many mAbs against membrane proteins, such as CCR3,¹⁰ CCR8,¹¹ CCR9,¹² CD19,¹³ CD20,^{14,15} CD44,^{16,17} CD133,¹⁸ EpCAM,^{19,20} HER2,²¹ HER3,²² KLRG1,²³ programmed cell death ligand 1 (PD-L1),²⁴ podoplanin (PDPN),^{25–36} TIGIT,³⁷ and TROP2^{38,39} using the Cell-Based Immunization and Screening (CBIS) method.

The CBIS method includes the immunization of antigen-overexpressed cells and high-throughput hybridoma screening using flow cytometry. In this study, a novel anti-mCD39 mAb was developed by the CBIS method.

Materials and Methods

Cell lines

Mouse leukemia SN36 was obtained from the Cell Resource Center for Biomedical Research Institute of Development, Aging and Cancer Tohoku University (Miyagi, Japan). LN229, Chinese hamster ovary (CHO)-K1, and P3X63Ag8U.1 (P3U1) were obtained from the American Type Culture Collection (Manassas, VA, USA).

The synthesized DNA (Eurofins Genomics KK) encoding mCD39 (Accession No.: NM_009848) was subsequently subcloned into a pCAGzeo_nPA-cRAPMAP vector, which is derived from a pCAGzeo vector (FUJIFILM Wako Pure Chemical Corporation, Osaka, Japan), N-terminal PA tag⁴⁰⁻⁴² and C-terminal RAP tag^{43,44} + MAP tag.^{45,46} The amino acid sequences of the tag system were as follows: PA tag, 12 amino acids (GVAMPGAEDDVV); RAP tag, 12 amino acids (DMVNPGLIEDRIE); and MAP tag, 12 amino acids (GDGMVPPGIEDK). The PA tag can be detected by an anti-human PDPN mAb (clone NZ-1).^{40-42,47-59} The mCD39 plasmid was transfected into CHO-K1 and LN229 cells, using a Neon transfection system (Thermo Fisher Scientific, Inc., Waltham, MA, USA). Stable transfectants were established through cell sorting using a cell sorter (SH800; Sony Corp., Tokyo, Japan), after which cultivation in a medium, containing 0.5 mg/mL of Zeocin (InvivoGen, San Diego, CA, USA) was performed.

SN36, CHO-K1, mCD39-overexpressed CHO-K1 (CHO/mCD39), and P3U1 were cultured in a Roswell Park Memorial Institute (RPMI)-1640 medium (Nacalai Tesque, Inc., Kyoto, Japan), with 10% heat-inactivated fetal bovine serum (FBS; Thermo Fisher Scientific, Inc.), 100 U/mL of penicillin, 100 µg/mL of streptomycin, and 0.25 µg/mL of amphotericin B (Nacalai Tesque, Inc.). LN229 and mCD39-overexpressed LN229 (LN229/mCD39) were cultured in Dulbecco's Modified Eagle Medium (DMEM) (Nacalai Tesque, Inc.), supplemented with 10% FBS, 100 U/mL of penicillin, 100 µg/mL streptomycin, and 0.25 µg/mL amphotericin B. All cells were grown in a humidified incubator at 37°C, at an atmosphere of 5% CO₂ and 95% air.

Production of hybridomas

A 5-week-old Sprague–Dawley rat was purchased from CLEA Japan (Tokyo, Japan). The animal was housed under specific pathogen-free conditions. All animal experiments were performed according to the relevant guidelines and regulations to minimize animal suffering and distress in the laboratory. The Animal Care and Use Committee of Tohoku University (Permit No.: 2019NiA-001) approved animal experiments. The rat was monitored daily for health during the complete 4-week duration of the experiment. A reduction of more than 25% of the total body weight was defined as a humane endpoint. During the sacrifice, the rat was euthanized through cervical dislocation, after which death was verified through respiratory and cardiac arrest.

To develop mAbs against mCD39, we intraperitoneally immunized one rat with LN229/mCD39 (1×10^9 cells) plus Inject Alum (Thermo Fisher Scientific, Inc.). The procedure included three additional injections every week (1×10^9 cells/rat), which were followed by a final booster intraperitoneal injection (1×10^9 cells/rat), 2 days before harvesting spleen cells. The harvested spleen cells were subsequently fused with P3U1 cells, using PEG1500 (Roche Diagnostics, Indianapolis, IN, USA), after which hybridomas were grown in the RPMI-1640 medium with 10% FBS, 100 U/mL of penicillin, 100 µg/mL of streptomycin, and 0.25 µg/mL of amphotericin B. For the hybridoma selection, hypoxanthine, aminopterin, and thymidine (HAT; Thermo Fisher Scientific, Inc.) were added into the medium. The supernatants were subsequently screened using flow cytometry using CHO/mCD39, CHO-K1, and SN36.

Antibodies

An anti-mCD39 mAb (clone 5F2, mouse IgG₁, kappa) was purchased from BioLegend (San Diego, CA, USA). Alexa Fluor 488-conjugated anti-rat IgG and Alexa Fluor 488-conjugated anti-mouse IgG secondary Abs were purchased from Cell Signaling Technology, Inc. (Danvers, MA, USA).

The cultured supernatant of C₃₉Mab-2-producing hybridomas was collected through centrifugation at 2330×g for 5 min, followed by filtration using Steritop (0.22 µm; Merck KGaA, Darmstadt, Germany). The filtered supernatants were subsequently applied to 1 mL of Protein G Sepharose 4 Fast Flow (GE Healthcare, Chicago, IL, USA). After washing with phosphate-buffered saline (PBS), bound antibodies were eluted with an IgG elution buffer (Thermo Fisher Scientific, Inc.), followed by immediate neutralization of eluates, using 1 M tris-HCl (pH 8.0). Finally, the eluates were concentrated, after which the elution buffer was replaced with PBS using Amicon Ultra (Merck KGaA).

Flow cytometric analysis

CHO-K1 and CHO/mCD39 were harvested after a brief exposure to 0.25% trypsin and 1 mM ethylenediaminetetraacetic acid (EDTA; Nacalai Tesque, Inc.). The cells were subsequently washed with 0.1% bovine serum albumin in PBS and treated with 0.001, 0.01, 0.1, and 1 µg/mL of primary mAbs for 30 min at 4°C. The cells were treated with Alexa Fluor 488-conjugated anti-rat IgG or Alexa Fluor 488-conjugated anti-mouse IgG (1:2000). The fluorescence data were collected using the SA3800 Cell Analyzer (Sony Corp.).

Determination of dissociation constant (K_D) by flow cytometry

CHO/mCD39 and SN36 were suspended in 100 µL serially diluted and C₃₉Mab-2 for 30 min at 4°C. The cells were treated with 50 µL of Alexa Fluor 488-conjugated anti-rat IgG (1:200). The fluorescence data were collected, using the SA3800 Cell Analyzer. The K_D was subsequently calculated by fitting saturation binding curves to the built-in; one-site binding models in GraphPad PRISM 8 (GraphPad Software, Inc., La Jolla, CA, USA).

Results and Discussion

We conducted flow cytometry using two anti-mCD39 mAbs: C₃₉Mab-2 and 5F2 against CHO/mCD39 and SN36

cell lines. C₃₉Mab-2 recognized CHO/mCD39 cells dose-dependently at 1, 0.1, 0.01, and 0.001 μg/mL (Fig. 1A). In contrast, 5F2 needed more than 0.01 μg/mL for the detection of CHO/mCD39 (Fig. 1A). Parental CHO-K1 cells were not recognized even at 1 μg/mL of all mAbs (Fig. 1B).

Furthermore, we investigated the reactivity of C₃₉Mab-2 against an endogenously mCD39-expressed cell line, SN36. C₃₉Mab-2 reacted with SN36 at more than 0.1 μg/mL (Fig. 1C). In contrast, 5F2 could react with SN36 at 1 μg/mL, but not at 0.1 μg/mL. These results suggested that C₃₉Mab-2 specifically recognizes mCD39 and is also useful for detecting endogenous mCD39 by flow cytometry.

To determine the K_D of C₃₉Mab-2 with mCD39-expressing cells, we conducted kinetic analysis by flow cytometry using CHO/mCD39 and SN36 cells. The geometric mean of the fluorescence intensity was plotted versus the concentration of C₃₉Mab-2. The K_D value of C₃₉Mab-2 for CHO/mCD39 was determined as 5.5×10^{-9} M (Fig. 2A). Furthermore, the K_D value of C₃₉Mab-2 for SN36 was determined as 4.9×10^{-9} M (Fig. 2B). These results indicate that C₃₉Mab-2 possess the high affinity for both CHO/mCD39 and SN36 cells.

Recently, Zhang *et al.*⁶⁰ demonstrated the application of an anti-mCD39 mAb for tumor therapy by the depletion of immunosuppressive cells through enhanced Fcγ receptor–

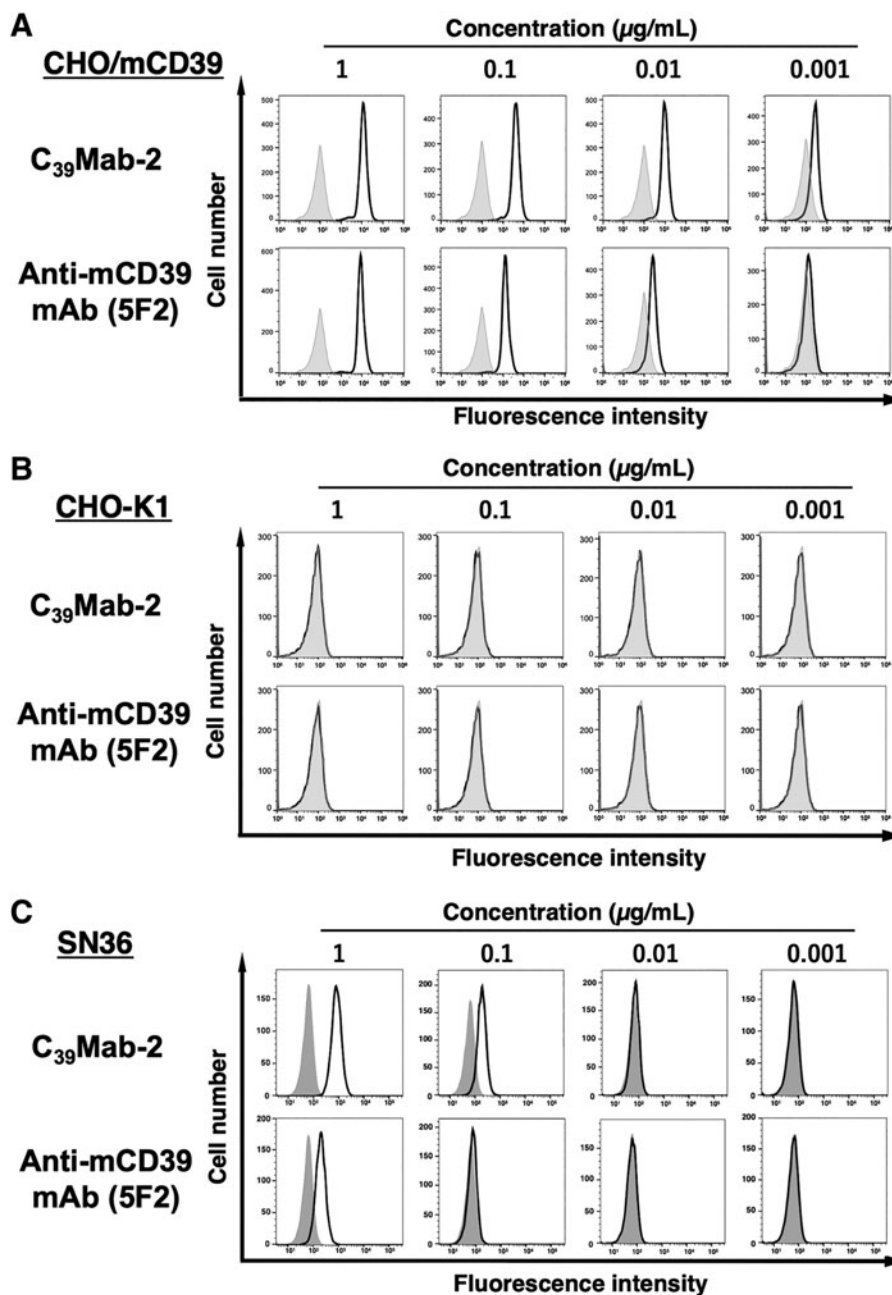


FIG. 1. Flow cytometry using anti-mCD39 mAbs. CHO/mCD39 (A), CHO-K1 (B), and SN36 (C) cells were treated with 0.001–1 μg/mL of C₃₉Mab-2 and 5F2, followed by treatment with Alexa Fluor 488-conjugated anti-rat IgG (for C₃₉Mab-2) or Alexa Fluor 488-conjugated anti-mouse IgG (for 5F2). The filled gray represents the negative control. CHO, Chinese hamster ovary; mAbs, monoclonal antibodies; mCD39, mouse CD39.

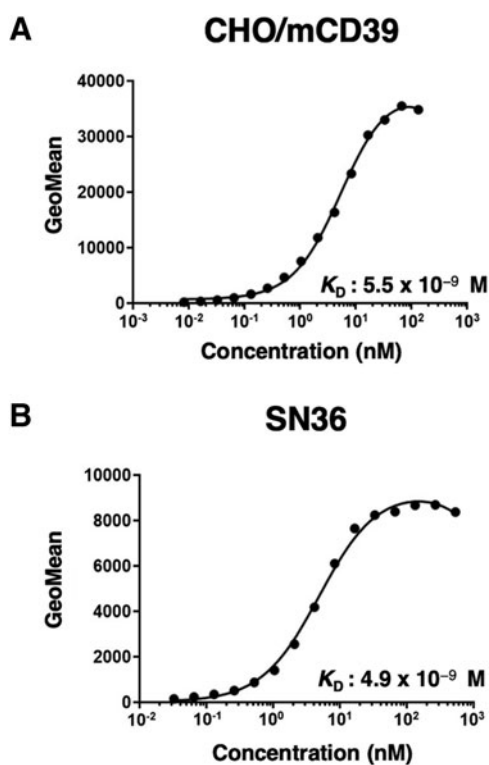


FIG. 2. The determination of the binding affinity of C₃₉Mab-2. CHO/mCD39 (A) and SN36 (B) cells were suspended in 100 μ L serially diluted C₃₉Mab-2 at the indicated concentrations. The cells were treated with Alexa Fluor 488-conjugated anti-rat IgG. The fluorescence data were subsequently collected using the SA3800 Cell Analyzer, following the calculation of the dissociation constant (K_D) by GraphPad PRISM 8.

mediated antibody-dependent cellular cytotoxicity (ADCC). They found that mCD39 expression on vascular endothelial cells and tumor-infiltrating immune cells was markedly higher than that in normal tissues. They used a non-neutralizing anti-mCD39 mAb (clone 5F2, mouse IgG₁) and screened an isotype-switched hybridoma subline of the IgG_{2c} isotype, which has more potent ADCC activities. To enhance the effector functions, the fucosyltransferase 8 (Fut8) gene was deleted in the 5F2 hybridomas to produce the defucosylated antibody. They showed that the defucosylated anti-mCD39 IgG_{2c} exerted the potent antitumor effect against mouse melanoma and colorectal tumor models through the depletion of regulatory/exhausted T cells, tumor-associated macrophages, and tumor vasculature with high mCD39 expression.

We previously produced recombinant antibodies, which were converted into mouse IgG_{2a} isotype from mouse IgG₁.^{61–68} Furthermore, we produced defucosylated IgG_{2a} mAbs using Fut8-deficient CHO-K1 cells to potentiate the ADCC activity.^{61–68} The defucosylated mAbs showed potent antitumor activity in mouse xenograft models.^{61–68} Therefore, an isotype-switched and defucosylated version of C₃₉Mab-2 could be used to evaluate the antitumor activity *in vivo*.

Author Disclosure Statement

No competing financial interests exist.

Funding Information

This research was supported in part by Japan Agency for Medical Research and Development (AMED) under Grant Numbers: JP23ama121008 (to Y.K.), JP23am0401013 (to Y.K.), 23bm1123027h0001 (to Y.K.), and JP23ck0106730 (to Y.K.), and by the Japan Society for the Promotion of Science (JSPS) Grants-in-Aid for Scientific Research (KAKENHI) Grant Numbers 22K06995 (to H.S.), 21K07168 (to M.K.K.), and 22K07224 (to Y.K.).

References

- Churov A, Zhulai G. Targeting adenosine and regulatory T cells in cancer immunotherapy. *Hum Immunol* 2021;82:270–278; doi: 10.1016/j.humimm.2020.12.005
- Vijayan D, Young A, Teng MWL, et al. Targeting immunosuppressive adenosine in cancer. *Nat Rev Cancer* 2017;17:709–724; doi: 10.1038/nrc.2017.86
- Sun C, Wang B, Hao S. Adenosine-A2A receptor pathway in cancer immunotherapy. *Front Immunol* 2022;13:837230; doi: 10.3389/fimmu.2022.837230
- Ohta A, Sitkovsky M. Role of G-protein-coupled adenosine receptors in downregulation of inflammation and protection from tissue damage. *Nature* 2001;414:916–920; doi: 10.1038/414916a
- Ohta A, Gorelik E, Prasad SJ, et al. A2A adenosine receptor protects tumors from antitumor T cells. *Proc Natl Acad Sci U S A* 2006;103:13132–13137; doi: 10.1073/pnas.0605251103
- Moesta AK, Li XY, Smyth MJ. Targeting CD39 in cancer. *Nat Rev Immunol* 2020;20:739–755; doi: 10.1038/s41577-020-0376-4
- Di Virgilio F, Sarti AC, Falzoni S, et al. Extracellular ATP and P2 purinergic signalling in the tumour microenvironment. *Nat Rev Cancer* 2018;18:601–618; doi: 10.1038/s41568-018-0037-0
- Li XY, Moesta AK, Xiao C, et al. Targeting CD39 in cancer reveals an extracellular ATP- and inflammasome-driven tumor immunity. *Cancer Discov* 2019;9:1754–1773; doi: 10.1158/2159-8290.Cd-19-0541
- Perrot I, Michaud HA, Giraudon-Paoli M, et al. Blocking antibodies targeting the CD39/CD73 immunosuppressive pathway unleash immune responses in combination cancer therapies. *Cell Rep* 2019;27:2411–2425.e2419; doi: 10.1016/j.celrep.2019.04.091
- Asano T, Nanamiya R, Takei J, et al. Development of anti-mouse CC chemokine receptor 3 monoclonal antibodies for flow cytometry. *Monoclon Antib Immunodiagn Immunother* 2021;40:107–112; doi: 10.1089/mab.2021.0009
- Tanaka T, Nanamiya R, Takei J, et al. Development of anti-mouse CC chemokine receptor 8 monoclonal antibodies for flow cytometry. *Monoclon Antib Immunodiagn Immunother* 2021;40:65–70; doi: 10.1089/mab.2021.0005
- Nanamiya R, Takei J, Asano T, et al. Development of anti-human CC chemokine receptor 9 monoclonal antibodies for flow cytometry. *Monoclon Antib Immunodiagn Immunother* 2021;40:101–106; doi: 10.1089/mab.2021.0007
- Yamada S, Kaneko MK, Sayama Y, et al. Development of novel mouse monoclonal antibodies against human CD19. *Monoclon Antib Immunodiagn Immunother* 2020;39:45–50; doi: 10.1089/mab.2020.0003
- Furusawa Y, Kaneko MK, Kato Y. Establishment of C(20)Mab-11, a novel anti-CD20 monoclonal antibody, for the detection of B cells. *Oncol Lett* 2020;20:1961–1967; doi: 10.3892/ol.2020.11753

15. Furusawa Y, Kaneko MK, Kato Y. Establishment of an anti-CD20 monoclonal antibody (C(20)Mab-60) for immunohistochemical analyses. *Monoclon Antib Immunodiagn Immunother* 2020;39:112–116; doi: 10.1089/mab.2020.0015
16. Ejima R, Suzuki H, Tanaka T, et al. Development of a novel anti-CD44 variant 6 monoclonal antibody C(44)Mab-9 for multiple applications against colorectal carcinomas. *Int J Mol Sci* 2023;24:4007; doi: 10.3390/ijms24044007
17. Yamada S, Itai S, Nakamura T, et al. Detection of high CD44 expression in oral cancers using the novel monoclonal antibody, C(44)Mab-5. *Biochem Biophys Rep* 2018;14:64–68; doi: 10.1016/j.bbrep.2018.03.007
18. Itai S, Fujii Y, Nakamura T, et al. Establishment of C(Mab)-43, a sensitive and specific anti-CD133 monoclonal antibody, for immunohistochemistry. *Monoclon Antib Immunodiagn Immunother* 2017;36:231–235; doi: 10.1089/mab.2017.0031
19. Li G, Suzuki H, Asano T, et al. Development of a novel anti-EpCAM monoclonal antibody for various applications. *Antibodies (Basel)* 2022;11:41; doi: 10.3390/antib11020041
20. Kaneko MK, Ohishi T, Takei J, et al. Anti-EpCAM monoclonal antibody exerts antitumor activity against oral squamous cell carcinomas. *Oncol Rep* 2020;44:2517–2526; doi: 10.3892/or.2020.7808
21. Itai S, Fujii Y, Kaneko MK, et al. H(2)Mab-77 is a sensitive and specific anti-HER2 monoclonal antibody against breast cancer. *Monoclon Antib Immunodiagn Immunother* 2017;36:143–148; doi: 10.1089/mab.2017.0026
22. Asano T, Ohishi T, Takei J, et al. Anti-HER3 monoclonal antibody exerts antitumor activity in a mouse model of colorectal adenocarcinoma. *Oncol Rep* 2021;46:173; doi: 10.3892/or.2021.8124
23. Asano T, Nanamiya R, Tanaka T, et al. Development of antihuman killer cell lectin-like receptor subfamily G member 1 monoclonal antibodies for flow cytometry. *Monoclon Antib Immunodiagn Immunother* 2021;40:76–80; doi: 10.1089/mab.2021.0008
24. Yamada S, Itai S, Nakamura T, et al. Monoclonal antibody L(1)Mab-13 detected human PD-L1 in lung cancers. *Monoclon Antib Immunodiagn Immunother* 2018;37:110–115; doi: 10.1089/mab.2018.0004
25. Yamada S, Itai S, Nakamura T, et al. P(Mab)-52: Specific and sensitive monoclonal antibody against cat podoplanin for immunohistochemistry. *Monoclon Antib Immunodiagn Immunother* 2017;36:224–230; doi: 10.1089/mab.2017.0027
26. Furusawa Y, Kaneko MK, Nakamura T, et al. Establishment of a monoclonal antibody P(Mab)-231 for tiger podoplanin. *Monoclon Antib Immunodiagn Immunother* 2019;38:89–95; doi: 10.1089/mab.2019.0003
27. Furusawa Y, Takei J, Sayama Y, et al. Development of an anti-bear podoplanin monoclonal antibody P(Mab)-247 for immunohistochemical analysis. *Biochem Biophys Rep* 2019;18:100644; doi: 10.1016/j.bbrep.2019.100644
28. Furusawa Y, Yamada S, Itai S, et al. Establishment of a monoclonal antibody P(Mab)-233 for immunohistochemical analysis against Tasmanian devil podoplanin. *Biochem Biophys Rep* 2019;18:100631; doi: 10.1016/j.bbrep.2019.100631
29. Goto N, Suzuki H, Tanaka T, et al. Development of a monoclonal antibody P(Mab)-292 against ferret podoplanin. *Monoclon Antib Immunodiagn Immunother* 2022;41(2):101–109; doi: 10.1089/mab.2021.0067
30. Furusawa Y, Yamada S, Itai S, et al. Establishment of monoclonal antibody P(Mab)-202 against horse podoplanin. *Monoclon Antib Immunodiagn Immunother* 2018;37:233–237; doi: 10.1089/mab.2018.0030
31. Kato Y, Yamada S, Furusawa Y, et al. P(Mab)-213: A monoclonal antibody for immunohistochemical analysis against pig podoplanin. *Monoclon Antib Immunodiagn Immunother* 2019;38:18–24.
32. Furusawa Y, Yamada S, Nakamura T, et al. P(Mab)-235: A monoclonal antibody for immunohistochemical analysis against goat podoplanin. *Heliyon* 2019;5:e02063; doi: 10.1016/j.heliyon.2019.e02063
33. Kato Y, Furusawa Y, Yamada S, et al. Establishment of a monoclonal antibody P(Mab)-225 against alpaca podoplanin for immunohistochemical analyses. *Biochem Biophys Rep* 2019;18:100633; doi: 10.1016/j.bbrep.2019.100633
34. Kato Y, Furusawa Y, Itai S, et al. Establishment of an anticetacean podoplanin monoclonal antibody P(Mab)-237 for immunohistochemical analysis. *Monoclon Antib Immunodiagn Immunother* 2019;38:108–113.
35. Kato Y, Furusawa Y, Sano M, et al. Development of an anti-sheep podoplanin monoclonal antibody P(Mab)-256 for immunohistochemical analysis of lymphatic endothelial cells. *Monoclon Antib Immunodiagn Immunother* 2020;39:82–90; doi: 10.1089/mab.2020.0005
36. Tanaka T, Asano T, Sano M, et al. Development of monoclonal antibody P(Mab)-269 against california sea lion podoplanin. *Monoclon Antib Immunodiagn Immunother* 2021;40:124–133; doi: 10.1089/mab.2021.0011
37. Takei J, Asano T, Nanamiya R, et al. Development of anti-human T cell immunoreceptor with Ig and ITIM domains (TIGIT) monoclonal antibodies for flow cytometry. *Monoclon Antib Immunodiagn Immunother* 2021;40:71–75; doi: 10.1089/mab.2021.0006
38. Sayama Y, Kaneko MK, Takei J, et al. Establishment of a novel anti-TROP2 monoclonal antibody Tr(Mab)-29 for immunohistochemical analysis. *Biochem Biophys Rep* 2021;25:100902; doi: 10.1016/j.bbrep.2020.100902
39. Tanaka T, Ohishi T, Asano T, et al. An anti-TROP2 monoclonal antibody Tr(Mab)-6 exerts antitumor activity in breast cancer mouse xenograft models. *Oncol Rep* 2021;46:132; doi: 10.3892/or.2021.8083
40. Tamura R, Oi R, Akashi S, et al. Application of the NZ-1 Fab as a crystallization chaperone for PA tag-inserted target proteins. *Protein Sci* 2019;28:823–836; doi: 10.1002/pro.3580
41. Fujii Y, Matsunaga Y, Arimori T, et al. Tailored placement of a turn-forming PA tag into the structured domain of a protein to probe its conformational state. *J Cell Sci* 2016;129:1512–1522; doi: 10.1242/jcs.176685
42. Fujii Y, Kaneko M, Neyazaki M, et al. PA tag: A versatile protein tagging system using a super high affinity antibody against a dodecapeptide derived from human podoplanin. *Protein Expr Purif* 2014;95:240–247; doi: 10.1016/j.pep.2014.01.009
43. Miura K, Yoshida H, Nosaki S, et al. RAP tag and P(Mab)-2 antibody: A tagging system for detecting and purifying proteins in plant cells. *Front Plant Sci* 2020;11:510444; doi: 10.3389/fpls.2020.510444
44. Fujii Y, Kaneko MK, Ogasawara S, et al. Development of RAP tag, a novel tagging system for protein detection and purification. *Monoclon Antib Immunodiagn Immunother* 2017;36:68–71; doi: 10.1089/mab.2016.0052
45. Fujii Y, Kaneko MK, Kato Y. MAP Tag: A novel tagging system for protein purification and detection. *Monoclon Antib Immunodiagn Immunother* 2016;35:293–299; doi: 10.1089/mab.2016.0039

46. Wakasa A, Kaneko MK, Kato Y, et al. Site-specific epitope insertion into recombinant proteins using the MAP tag system. *J Biochem* 2020;168:375–384; doi: 10.1093/jb/mvaa054
47. Kato Y, Kaneko MK, Kuno A, et al. Inhibition of tumor cell-induced platelet aggregation using a novel anti-podoplanin antibody reacting with its platelet-aggregation-stimulating domain. *Biochem Biophys Res Commun* 2006;349:1301–1307; doi: 10.1016/j.bbrc.2006.08.171
48. Chalise L, Kato A, Ohno M, et al. Efficacy of cancer-specific anti-podoplanin CAR-T cells and oncolytic herpes virus G47Delta combination therapy against glioblastoma. *Mol Ther Oncolytics* 2022;26:265–274; doi: 10.1016/j.omto.2022.07.006
49. Ishikawa A, Waseda M, Ishii T, et al. Improved anti-solid tumor response by humanized anti-podoplanin chimeric antigen receptor transduced human cytotoxic T cells in an animal model. *Genes Cells* 2022;27:549–558; doi: 10.1111/gtc.12972
50. Tamura-Sakaguchi R, Aruga R, Hirose M, et al. Moving toward generalizable NZ-1 labeling for 3D structure determination with optimized epitope-tag insertion. *Acta Crystallogr D Struct Biol* 2021;77:645–662; doi: 10.1107/S2059798321002527
51. Kaneko MK, Ohishi T, Nakamura T, et al. Development of core-fucose-deficient humanized and chimeric anti-human podoplanin antibodies. *Monoclon Antib Immunodiagn Immunother* 2020;39:167–174; doi: 10.1089/mab.2020.0019
52. Abe S, Kaneko MK, Tsuchihashi Y, et al. Antitumor effect of novel anti-podoplanin antibody NZ-12 against malignant pleural mesothelioma in an orthotopic xenograft model. *Cancer Sci* 2016;107:1198–1205; doi: 10.1111/cas.12985
53. Kaneko MK, Abe S, Ogasawara S, et al. Chimeric anti-human podoplanin antibody NZ-12 of lambda light chain exerts higher antibody-dependent cellular cytotoxicity and complement-dependent cytotoxicity compared with NZ-8 of kappa light chain. *Monoclon Antib Immunodiagn Immunother* 2017;36:25–29; doi: 10.1089/mab.2016.0047
54. Ito A, Ohta M, Kato Y, et al. A real-time near-infrared fluorescence imaging method for the detection of oral cancers in mice using an indocyanine green-labeled podoplanin antibody. *Technol Cancer Res Treat* 2018;17:1533033818767936; doi: 10.1177/1533033818767936
55. Shiina S, Ohno M, Ohka F, et al. CAR T cells targeting podoplanin reduce orthotopic glioblastomas in mouse brains. *Cancer Immunol Res* 2016;4:259–268; doi: 10.1158/2326-6066.CIR-15-0060
56. Kuwata T, Yoneda K, Mori M, et al. Detection of circulating tumor cells (CTCs) in malignant pleural mesothelioma (MPM) with the “Universal” CTC-Chip and an anti-podoplanin antibody NZ-1.2. *Cells* 2020;9:888; doi: 10.3390/cells9040888
57. Nishinaga Y, Sato K, Yasui H, et al. Targeted phototherapy for malignant pleural mesothelioma: Near-infrared photoimmunotherapy targeting podoplanin. *Cells* 2020;9:1019; doi: 10.3390/cells9041019
58. Kato Y, Kaneko MK, Kunita A, et al. Molecular analysis of the pathophysiological binding of the platelet aggregation-inducing factor podoplanin to the C-type lectin-like receptor CLEC-2. *Cancer Sci* 2008;99:54–61; doi: 10.1111/j.1349-7006.2007.00634.x
59. Kato Y, Vaidyanathan G, Kaneko MK, et al. Evaluation of anti-podoplanin rat monoclonal antibody NZ-1 for targeting malignant gliomas. *Nucl Med Biol* 2010;37:785–794; doi: 10.1016/j.nucmedbio.2010.03.010
60. Zhang H, Feng L, de Andrade Mello P, et al. Glycoengineered anti-CD39 promotes anticancer responses by depleting suppressive cells and inhibiting angiogenesis in tumor models. *J Clin Invest* 2022;132:e157431; doi: 10.1172/jci157431
61. Li G, Suzuki H, Ohishi T, et al. Antitumor activities of a defucosylated anti-EpCAM monoclonal antibody in colorectal carcinoma xenograft models. *Int J Mol Med* 2023;51:18; doi: 10.3892/ijmm.2023.5221
62. Nanamiya R, Takei J, Ohishi T, et al. Defucosylated anti-epidermal growth factor receptor monoclonal antibody (134-mG(2a)-f) exerts antitumor activities in mouse xenograft models of canine osteosarcoma. *Monoclon Antib Immunodiagn Immunother*. 2022;41:1–7; doi: 10.1089/mab.2021.0036
63. Kawabata H, Suzuki H, Ohishi T, et al. A defucosylated mouse anti-CD10 monoclonal antibody (31-mG(2a)-f) exerts antitumor activity in a mouse xenograft model of CD10-overexpressed tumors. *Monoclon Antib Immunodiagn Immunother* 2022;41:59–66; doi: 10.1089/mab.2021.0048
64. Kawabata H, Ohishi T, Suzuki H, et al. A defucosylated mouse anti-CD10 monoclonal antibody (31-mG(2a)-f) exerts antitumor activity in a mouse xenograft model of renal cell cancers. *Monoclon Antib Immunodiagn Immunother* 2022;41(6):320–327; doi: 10.1089/mab.2021.0049
65. Asano T, Tanaka T, Suzuki H, et al. A defucosylated anti-EpCAM monoclonal antibody (EpMab-37-mG(2a)-f) exerts antitumor activity in Xenograft Model. *Antibodies (Basel)* 2022;11(4):74; doi: 10.3390/antib11040074
66. Tateyama N, Nanamiya R, Ohishi T, et al. Defucosylated anti-epidermal growth factor receptor monoclonal antibody 134-mG(2a)-f exerts antitumor activities in mouse xenograft models of dog epidermal growth factor receptor-overexpressed cells. *Monoclon Antib Immunodiagn Immunother* 2021;40:177–183; doi: 10.1089/mab.2021.0022
67. Takei J, Ohishi T, Kaneko MK, et al. A defucosylated anti-PD-L1 monoclonal antibody 13-mG(2a)-f exerts antitumor effects in mouse xenograft models of oral squamous cell carcinoma. *Biochem Biophys Res Commun* 2020;524:100801; doi: 10.1016/j.bbrc.2020.100801
68. Takei J, Kaneko MK, Ohishi T, et al. A defucosylated antiCD44 monoclonal antibody 5mG2af exerts antitumor effects in mouse xenograft models of oral squamous cell carcinoma. *Oncol Rep* 2020;44:1949–1960; doi: 10.3892/or.2020.7735

Address correspondence to:

Yukinari Kato
 Department of Antibody Drug Development
 Tohoku University Graduate School of Medicine
 2-1, Seiryomachi, Aoba-ku
 Sendai
 Miyagi 980-8575
 Japan

E-mail: yukinari.kato.e6@tohoku.ac.jp

Received: September 15, 2023

Accepted: November 9, 2023